

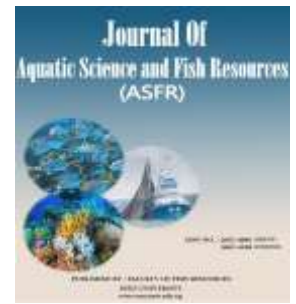


Aquatic Science and Fish Resources

<http://asfr.journals.ekb.eg>

Print ISSN: 2682-4086

Online ISSN: 2682-4108



Water Temperature Modeling for Water Tank in Recirculating Aquaculture System for Raising Nile Tilapia

Ahmed M. Ragab^{1,*}, Abdel-Ghany M. El-Gindy^{2,3}, Osama Kaddour¹, Samir Ahmad Ali⁴

¹ Engineering Science Department, Faculty of Fish Resources, Suez University, Suez, Egypt.

² Agricultural Engineering Department, Faculty of Agriculture, Ain Shams University, Egypt.

³ Faculty of Desert Agriculture, King Salman International University, Ras Sudr, Egypt.

⁴ Agricultural and Bio-systems Engineering Department, Faculty of Agriculture, Benha University, Qalyubiyya, Egypt.

ARTICLE INFO

Article history:

Received Aug. 1,2022

Received in revised form Aug. 27,2022

Accepted Aug. 30,2022

Available online Sept. 1,2022

Keywords

Recirculating aquaculture system,

Heat balance,

Energy modeling,

Solar radiation

ABSTRACT

Temperature control presents a high cost for recirculating aquaculture systems (RAS). It is necessary to find a solution that would save energy in RAS. A heat balance for recirculating aquaculture system was developed on python program and a heat predicting model on graphic interface user (GUI) was produced with the given name of RAS designer and operation assistant. The model can predict precisely the heat energy required to be added or removed to maintain the water temperature at optimum water temperature to guarantee fish welfare and productivity. The model was validated by comparing predicted heat energy to actual heat energy. The model can predict the total annual, monthly, daily, hourly and extreme condition heating requirements, solar radiation, and water temperature. The predicted temperature of the water in the tank by the model ranged from 21.96 °C to 33.26 °C with an average of 27.92 °C ± 1.34 °C. on the other hand the actual temperature of the water in the tank ranged from 22.20°C to 30.90°C with an average of 28.41 °C ± 1.16 °C. The model gives good and promising results that are relatively realistic.

1. Introduction

The main environmental factor influencing the growth and development of aquatic species is the water temperature. It must be maintained within a physiologically acceptable range to achieve year-round aquaculture output. Placement of the production units inside covered facilities where the impact of weather on the air and water is minimized is a typical method for accomplishing this (Li *et al.*, 2009).

The cost of heating a greenhouse in the winter, especially given the high cost of energy today, is substantial. Because heating expenses make up a sizeable amount of the total energy requirements for recirculating aquaculture productions, correct heating

cost aquaculture productions, correct heating cost estimation is crucial to ensuring the viability of a proposed system from an economic standpoint (Singh and Marsh, 1996).

Exploring potential management strategies for current systems through simulation is crucial to ensuring profitability by lowering heat loss and related heating expenses (Li *et al.*, 2009).

It has taken a lot of effort to model greenhouse tanks or pond systems (Zhu *et al.*, 1998; Sarkar and Tiwari 2006; Jain, 2007; Li *et al.*, 2009; Davison and Piedrahita, 2015). Typical model inputs for simulating a greenhouse-covered aquaculture system include weather information such as air temperature, solar radiation, humidity, and wind speed (Zhu *et al.*, 1998; Sarkar and Tiwari 2006; Jain, 2007; Li *et al.*, 2009; Davison and Piedrahita, 2015). Depending on the location, these data can either be measured by an on-site weather station or collected from several public data sources. When aeration is occurring at high rates

** Corresponding author: at Suez University

E-mail addresses: ahmed.ragab@suezuni.edu.eg

.doi: [10.21608/ASFR.2022.157366.102](https://doi.org/10.21608/ASFR.2022.157366.102)

compared to the volume of water, modeling heat transfer may be crucial to take into account. (Talati and Stenstrom, 1990; Sedory, 1992; Makinia et al., 2005). Since the models are based on greenhouses, they lack the flexibility to add and remove a cover daily and do not take into account the significance of any aeration effects that might be present in a system that is strongly aerated (Davison and Piedrahita, 2015). In their 2015 study, Davison and Piedrahita (2015) showed that a basic cover and insulation are insufficient to increase the tank's temperature throughout the winter to the level necessary for ideal growing conditions. Nevertheless, a cover may enable ideal growing conditions during other seasons when more sunlight is available, such as early spring and late fall, or it may lower costs if additional heating is necessary during the winter.

Ali (2006) concluded that the two main sources of energy for ponds were solar radiation and longwave sky radiation. Average contributions from solar radiation and longwave sky radiation were 33% and 21%, respectively (with a range of 14-49% and 0-51%).

Li et al. (2009) evaluated the differences between the real and expected values and concluded that the model accurately depicts the system, with average absolute errors of 1.4%, 0.5%, and 8% for the prediction of air temperature, water temperature, and relative humidity, respectively.

Ali (2012) developed a model to forecast solar radiation. Solar radiation peaked at 2402.98 W on an average winter day, compared to 3931.91 W on an average summer day.

Khater (2012) showed that the system's measurements of the water's temperature ranged from 25 to 30.90 C. However, the program predicted it would range from 24.20 C to 29.86 C.

Davison and Piedrahita (2015) developed a model to estimate *G. Pacifica* growing conditions, the model frequently predicts values that are within 0.3°C of the measured values. In the best-case scenario, a system with insulation with a thermal resistance of at least 0.2 m² °C W and a high-performance cover that boosts shortwave radiation transmission while decreasing longwave radiation transmission experienced an increase in temperature of about 3 °C.

Ragab et al. (2022) have developed a mass balance concerning oxygen and ammonia and a GUI has been produced. As a work completion, a heat balance must be done to cover the most important parameters in the RASs.

The objective of this study was to construct and verify a heat-predicting model of a recirculating aquaculture system for growing Nile tilapia that predicts tank water temperature to influence system design and operating decisions to maximize Nile tilapia growth. The model consists of all heat vectors that have impact on water temperature. The model is very important in designing and calculating the heat energy required to be added or removed to design the heat exchanger.

MATERIALS AND METHODS

2.1. Model development

The energy balance equation of the water in the tank is (Li et al., 2009; Davison and Piedrahita, 2015):

$$C_w V_w \frac{dT_w}{dt} = q_{sw} - q_{Vw,i} - q_{Lw,i} + q_{Rc1,w} + q_{Rc2,w} - q_{Rw,sky} - q_{Dw,s} - q_{Vw,at} - q_{Lw,at} - q_{Lw,sw} + q_{other} \quad (1)$$

where

C_w is the specific heat of the water on a volumetric basis (J m⁻³ °C⁻¹)

V_w is the volume of the water (m³)

T_w is the water temperature (°C)

t is time (s)

q_{sw} is the solar radiation absorbed by water (W)

$q_{Vw,i}$ is the sensible heat transfer between the water surface and the inside air (W)

$q_{Lw,i}$ is the latent heat loss from the evaporation of the tank water (W)

$q_{Rc1,w}$ is the net thermal radiation between the water surface and the exterior cover

$q_{Rc2,w}$ is the net thermal radiation between the water surface and the interior cover

$q_{Rw,sky}$ is the net thermal radiation between the water surface and the sky (W)

$q_{Dw,s}$ is the conduction between the tank and the soil at the bottom of the tank

$q_{Vw,at}$ is the sensible heat transfer between the water and the aeration bubbles (W)

$q_{Lw,at}$ is the latent heat transfer between the water and the aeration bubbles (W)

$q_{lw,sw}$ is the latent heat transfer between the water and the ambient air due to swirling water motion (W)

q_{other} is the heat transfer due to inlet water addition or removal and rain if present (W)

According to **Li et al. (2009)** the sensible heat transfer between ambient air and the surface of the water:

$$q_{Vw,i} = h_{Vw,i} A_w (T_w - T_i) \quad (2)$$

Where

$h_{Vw,i}$ is the convective coefficient between the water surface and the inside air ($W m^{-2} \text{ } ^\circ C^{-1}$)

A_w is water area (m^2)

T_i is inside air temperature ($^\circ C$).

The convective coefficient between the water surface and the inside air could be determined (**Papadakis et al., 1992**).

$$h_{Vw,i} = c_4 |T_w - T_i|^{0.33}$$

(3)

Where

C_4 Coefficient (=3 according to **Li et al. (2009)**)

Li et al. (2009) calculated the latent heat loss from the evaporation of the water (W):

$$q_{hw,i} = h_{hw,i} A_w (e_w^* - e_i) \quad (4)$$

Where

$h_{hw,i}$ is the convective coefficient for latent heat between the water surface and the inside air ($W m kg^{-1}$)

e_i is the water vapor concentration of the inside air ($kg m^{-3}$)

e_w^* is the saturated water vapor concentration at water temperature ($kg m^{-3}$)

Li et al. (2009) determine the convective coefficient for latent heat by the next equation:

$$h_L = \frac{\lambda}{c_a} Le^{1/3} h_V \quad (5)$$

Where

λ is the latent heat of water evaporation ($J kg^{-1}$)

c_a is the specific heat of the air on a volumetric basis ($J m^{-3} \text{ } ^\circ C^{-1}$)

Le is Lewis number representing the ratio of thermal diffusivity to mass diffusivity = 0.89 (**Zhu et al., 1998**).

The solar radiation absorbed by the water was calculated (**Davison and Piedrahita, 2015**) as:

$$q_{sw} = \tau_{S,c}^2 (1 - \rho_{S,w}) A_w S \quad (6)$$

Where

$\tau_{S,c}$ is the transmissivity of a single layer of plastic cover to solar radiation

$\rho_{S,w}$ is the reflectivity of water surface

S is the outside global solar radiation ($W m^{-2}$).

The following formulae can be used to calculate the amount of incoming extraterrestrial radiation

Where

ω_{time} is the solar time (degrees)

(**Khater, 2012**):

$$S = \Psi S_c \left(\frac{D}{D_0}\right)^2 \cos \theta_z \quad (7)$$

Where

Ψ is a "clearness" factor (1 on clear days, 0.2 on cloudy days)

S_c is the solar constant ($1353 W m^{-2}$)

D is the distance from the Earth to the sun (km)

D_0 is the mean distance from the Earth to the sun, 1.496×10^8 km

θ_z is the solar zenith (degrees)

The next equation is used to determine the squared ratio between the distances from the Earth to the sun to the mean distance from the Earth to the sun (**Ali, 2006**):

$$\left(\frac{D}{D_0}\right)^2 = 1.000110 + 0.034221 \cos \tau + 0.001280 \sin \tau + 0.000719 \cos(2\tau) + 0.000077 \sin(2\tau) \quad (8)$$

Where

τ is the day angle (radians)

The day angle equation is (**Duffie et al., 2020**):

$$\tau = \frac{2\pi(n-1)}{365} \quad (9)$$

Where

n is the day of the year (on January 1st, $n = 1$)

Duffie et al. (2020) concluded that the cosine zenith angle could be calculated as:

$$\cos \theta_z = \sin \Phi \sin \delta + \cos \Phi \cos \delta \cos \omega \quad (10)$$

Where

Φ is the pond's latitude (positive for north) (degrees)

δ is the solar declination (the angle formed by the line from the center of the earth to the center of the sun and the earth's equator) (degrees)

ω is the hour angle (degrees)

ω_{time} is the solar time (degrees)

According to **ASHRAE (2009)**, the following equation is used to compute the solar declination:

$$\delta = 23.45 \sin \left[\frac{360}{365} (284 + n) \right] \quad (11)$$

The hour angle could be determined according to **Duffie et al. (2020)**:

$$\omega = (12 - \omega_{time}) \times 15^\circ \quad (12)$$

The solar time could be calculated according to the equation (**ASHRAE, 2009**):

$$\omega_{time} = LST + (Lnt - Lng) \div 15 \quad (13)$$

Where

LST is the local standard time

Lnt is the longitude of the standard time meridian (degrees)

Lng is the longitude of the pond (degrees)

The net thermal radiation between the surface of the water and the exterior cover (**Li et al., 2009**):

$$q_{Rc1,w} = \frac{\sigma \cdot \tau_{c2} A_w}{\epsilon_w^{-1} + \epsilon_c^{-1} - 1} [(T_{c1} + 273.16)^4 - (T_w + 273.16)^4] \quad (14)$$

Where

σ is the Stefan–Boltzmann constant = 5.67×10^{-8}

τ_{c2} is the transmissivity of a single layer of plastic cover to solar radiation

ϵ_w is the emissivity of the water surface

ϵ_c is the emissivity of the interior surface of the exterior cover

T_{c1} is the exterior greenhouse cover temperature ($^\circ\text{C}$) and T_w is the water temperature ($^\circ\text{C}$).

The net thermal radiation between the water surface and the interior cover (**Li et al., 2009**):

$$q_{Rc2,w} = \frac{\sigma A_w}{\epsilon_w^{-1} + \epsilon_{c2}^{-1} - 1} [(T_{c2} + 273.16)^4 - (T_w + 273.16)^4] \quad (15)$$

Where

ϵ_w is the emissivity of the water surface

ϵ_{c2} is the emissivity of the interior surface of the interior cover

T_{c2} is the interior greenhouse cover temperature ($^\circ\text{C}$) and T_w is the water temperature ($^\circ\text{C}$).

Assuming the sky is a black body, the net thermal radiation between the water surface and the sky is (**Li et al., 2009**):

$$q_{Rw,sky} = \sigma \cdot \epsilon_w \cdot \tau_{c1} \cdot \tau_{c2} A_w [(T_w + 273.16)^4 - (T_{sky} + 273.16)^4] \quad (16)$$

Where

τ_{c1} is the transmissivity of the exterior cover for thermal radiation

T_{sky} the sky temperature ($^\circ\text{C}$)

The sky temperature could be determined by the next equation (**Swinbank, 1963**):

$$T_{sky} = 0.0552(T_o + 273.16)^{1.5} - 273 \quad (17)$$

Where

T_o is the outside air temperature ($^\circ\text{C}$)

The conductive heat transfer between the tank and the soil beneath is (**Li et al., 2009**):

$$q_{Dw,s} = \frac{k_s}{l_s} A_w (T_w - T_s) \quad (18)$$

Where

k_s is the thermal conductivity of soil ($\text{W m}^{-1} \text{ }^\circ\text{C}^{-1}$)

l_s is the thickness of the soil layer where the temperature at its bottom can be regarded as constant (m)

T_s is the soil temperature ($^\circ\text{C}$)

The heat transfer between the water in the tank and the air through the tank sides and bottom if the bottom of the tank is above the ground (**Davison and Piedrahita, 2015**):

$$q_{Dw,i} = A_{sb} \frac{1}{Res_T} (T_w - T_i) \quad (19)$$

Where

A_{sb} is the surface area of the sides and bottom of the tank (m^2)

Res_T is the total thermal resistance of the tank ($\text{m}^2 \text{ }^\circ\text{C w}^{-1}$)

The total thermal resistance of the tank if the bottom of the tank is above the ground (**Davison and Piedrahita, 2015**):

$$Res_T = \left(\frac{1}{h_i} \right) + (Res_{T,wall}) + \left(\frac{1}{h_w} \right) \quad (20)$$

(20)

Where

h_i is the convective heat transfer between the wall and the bottom of the tank with air ($\text{w m}^{-2} \text{ }^\circ\text{C}^{-1}$)

Res_T is the total thermal resistance of the tank plus insulation if present ($\text{m}^2 \text{ }^\circ\text{C w}^{-1}$)

h_w is the convective heat transfer between water and the wall and the bottom of the tank ($\text{w m}^{-2} \text{ }^\circ\text{C}^{-1}$)

The next equation was used to calculate sensible heat transfer between the water and the aeration bubbles (**Davison and Piedrahita, 2015**):

$$q_{Vw,at} = Q_{air} \rho_{ai} C_{p_{ai}} (T_w - T_{ai}) \quad (21)$$

Where

Q_{air} is the rate of aeration airflow ($\text{m}^3 \text{ s}^{-1}$)

ρ_{ai} is the density of aeration inlet air(kg m⁻³)
 $C_{p_{ai}}$ is the specific heat of aeration inlet air(J kg⁻¹ °C⁻¹)
 T_{ai} is aeration inlet air temperature (°C)

Sedory (1992) calculated the latent heat transfer between the water and the aeration bubbles as:

$$q_{Lw,at} = \frac{M_w Q_{air} \lambda}{100R} \left(\frac{P_w (Rh_a + h_f(100 - Rh_a))}{T_w + 273} - \frac{P_{ai} Rh_{ai}}{T_{ai} + 273} \right) \quad (22)$$

Where

M_w is the molecular weight of water (kg kmol⁻¹)
 R is the universal gas constant (J kmol⁻¹K⁻¹)
 Rh_{ai} is the relative humidity of ambient air, measured by the weather station (%)
 P_w is the vapor pressure at a temperature of water (Pa)

Talati and Stenstrom (1990) computed the latent heat transfer between the water and the ambient air due to swirling water motion (W) as:

$$q_{Lw,sw} = \left(1.145 \times 10^6 \left(1 - \frac{Rh_a}{100} \right) + 6.86 \times 10^4 (T_w - T_i) \right) \times 2.171828^{0.604 T_a} V_{sw} A_W^{0.95} C \quad (23)$$

The heat transfer due to inlet water addition, rain,

Where

V_{sw} is the velocity of water surface caused by aeration swirling, a constant value(m s⁻¹)
 C constant for converting from English to SI units (W day cal⁻¹)

and outlet water drainage (**Davison and Piedrahita, 2015**):

$$q_{other} = Q_{wat} C_{p_{wi}} \rho_{wi} (T_w - T_{wi}) \quad (24)$$

Where

Q_{wat} is the rate of water flow (m³s⁻¹)
 $C_{p_{wi}}$ is the heat capacity of, inlet, rain, or outlet water (J kg⁻¹°C⁻¹)
 ρ_{wi} is the density of inlet water (kg m⁻³)
 T_{wi} is the inlet, rain, or outlet water temperature (°C)

2.2 Analysis Procedures

2.2.1 The model description

Python version 3.8.6 was used to create the model. It determines the expected tank

temperature as well as the amount of energy being transmitted through various heat transfer mechanisms. This model's flowchart is shown in fig. 1.

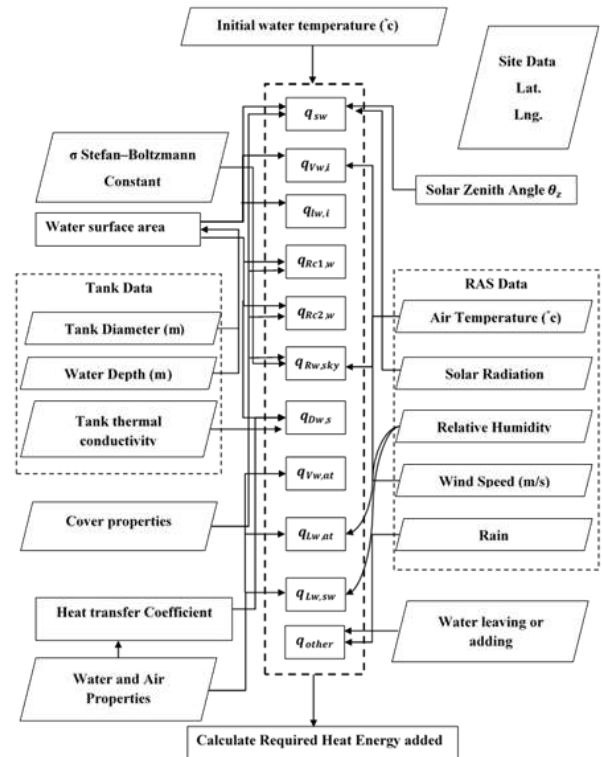


Fig. 1. The flowchart for energy balance for water tank in Recirculating aquaculture system for Nile tilapia raising

To make the model more understandable, the following presumptions were used:

Despite variations in water temperature, the water's density and specific heat remained constant. Since there was a less than 1% difference in density between 273K and 316.3K, this was a realistic assumption to make. The specific heat changes relatively by 1.2% from 4.225 kJ kg⁻¹ K⁻¹ at 273K to 4.174 kJ kg⁻¹ K⁻¹ at 316.3K.

Tank volume remained steady. It seemed logical to assume that water was constantly being released from the standpipe. The tank's capacity stayed constant. It appeared logical to think that water was being released from the standpipe continuously.

The sky was clear to calculate the emitted atmospheric longwave radiation).

The characteristics of the soil beneath the tank were evenly distributed. The fact that the soil beneath the water tank's floor was compacted and completely saturated with water provided support

for this idea. Another assumption is when the relative humidity of the air is around 100%, there is no evaporation. Insignificant amounts of heat were produced by the degrading of microorganisms in the water tank. The parameters used in this model are shown in table 1.

Table 1. Parameters used in the model

	Symbol	Value	Unit	Source
Cover	ϵ_c	0.53		Zhu <i>et al.</i> (1998)
	τ_c	0.42		
	$\tau_{s,c}$	0.8		
Air	Ca	1185	$J m^3 ^\circ C^{-1}$	Lienhard and Lienhard (2003)
Soil	k_s	1.8	$W m^{-1} ^\circ C^{-1}$	Li <i>et al.</i> (2009)
	l_s	1.5	m	
Water	Cw	4.17×10^6	$J m^3 ^\circ C^{-1}$	Lienhard and Lienhard (2003)
	$\rho_{s,w}$	0.1		Zhu <i>et al.</i> (1998)
	λ	2.26×10^6	$J kg^{-1}$	Davison and Piedrahita
	Mw	18	$Kg/k mol$	Piedrahita
	R	8.314	$J kg^{-1}$	(2015)

2.3. Experimental procedures

2.3.1. Model Validation

Weather data were obtained from the weather station at the Faculty of Agriculture Moshtohor, Benha University, Egypt (latitude $30^\circ 21' N$ and $31^\circ 13' E$). It was used for the model validation concerning solar radiation. The data of the four seasons; autumn 2016, winter 2017, spring 2017, and summer 2017; was used. The fifteenth days of the first month in each season were selected for solar radiation validation as a table 2 shows. It was used also for the model application and experimentation. The data used for the model validation and application in this paper are based on data from Benha University, Faculty of Agriculture, RAS Project (Khater, 2012).

Table 2. Days used in validation

Year	Season	Month	Day	Cloudiness
2016	Autumn	October	15	0.3
2017	Winter	January	15	0.5

2017	Spring	April	15	0.6
2017	Summer	July	15	0.8

2.4. Programming language:

Python 3.8.6. was used to construct the model. Matplotlib (V. 3.0.3), Numpy (V. 1.16.2), Tkinter (V. 8.6), and Math (V. 1.2) packages had been installed and used. Anaconda application also has been used to make python use easier. MS Excel 2007 was also used to compare the data of the model and the Weather data. It was also used for comparing expected and actual data and for checking the model working well.

RESULTS

3.1. The RAS design and operation assistant GUI

The energy balance input screen consists of buttons for inputs. The inputs include weather data such as air temperature and air humidity. The clearness factor is included. The site latitude and longitude are also included. The water tank depth and diameter. Other buttons for an hour, day, and month input. An optional button for covers number or no greenhouse system. Another button for water set temperature. Calculate button is in the middle of the screen bottom. Other input data is included. It is shown in fig. 2.

Fig. 2. Energy balance inputs screen

3.2. Weather data

Fig. 3 illustrates the weather data on an hourly basis. It includes the Solar radiation $W m^{-2}$, air temperature $^\circ C$, relative humidity, and wind speed $m s^{-1}$. Diurnal variations are shown during day hours.

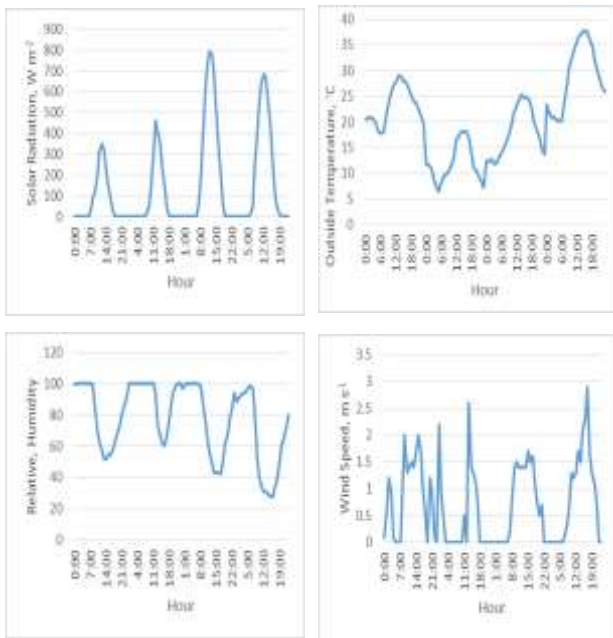


Fig. 3. outside weather: Solar radiation, air temperature, relative humidity, and wind speed

3.3. Model experimentations

3.3.1. Solar radiation

3.3.1.1. Solar radiation on the outdoor water tank

It was also from 244 w m^{-2} at 7 am to 69 w m^{-2} at 5 pm and reached 749 w m^{-2} at noon on 15/4/2017 (spring). It ranged from 180 w m^{-2} at 6 am to 5 w m^{-2} at 7 pm and reached 1032 w m^{-2} at noon on 15/7/2017 (summer). These results are shown clearly in fig. 4.

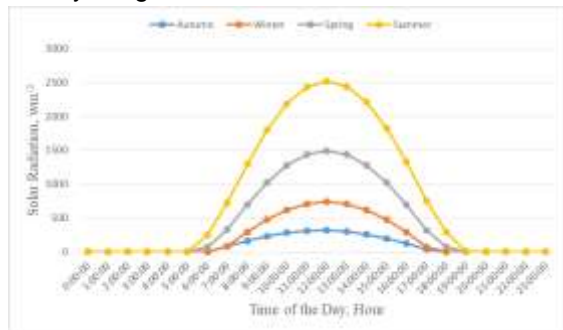


Fig. 4. Predicted hourly average solar radiation during four days in different seasons.

3.3.1.2. Solar radiation on the outdoor and inside the greenhouse water tank

It is apparent in fig. 5 that the solar radiation incident on water surface in outdoor recirculating

aquaculture tank is the highest when compared to the one-cover and two-cover greenhouse systems during the sunlight hours (at all seasons). It is also visible that the solar radiation incident on water surface in recirculating aquaculture tank under greenhouse with one-cover is more than the solar radiation incident on water surface in recirculating aquaculture tank under greenhouse with two-cover systems during the sunlight hours (at all seasons).

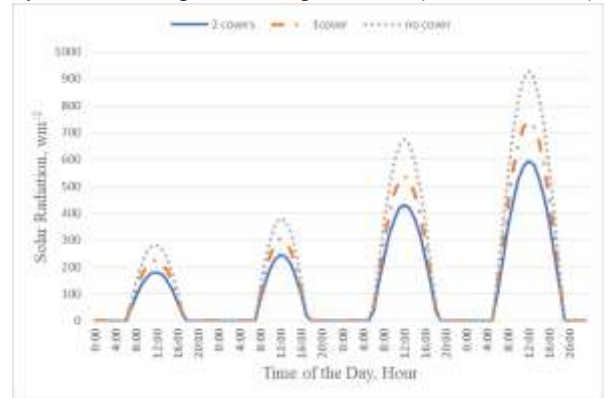


Fig. 5. Predicted hourly average solar radiation incident on one squared meter of water in outdoor and inside greenhouse systems.

3.3.2. Sky radiation

Fig. 6 clearly illustrates that the sky radiation from the water surface in the outdoor recirculating aquaculture tank is the highest when compared to the one-cover and two-cover greenhouse systems during day hours (at all seasons). Additionally, sky radiation from the water surface in recirculating aquaculture tank under a greenhouse with one cover is more than the solar radiation incident on the water surface in recirculating aquaculture tank under a greenhouse with two-cover systems during day hours (at all seasons).

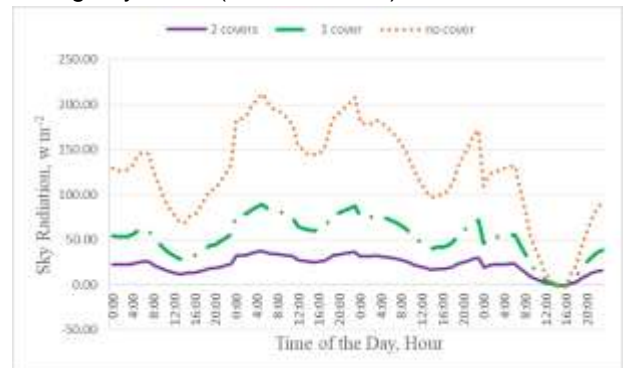


Fig. 6. Predicted hourly sky radiation from one squared meter of water in outdoor and inside greenhouse system.

3.4. Model validation

3.4.1 Solar radiation

A comparison between the actual solar radiation available on the selected four days of October, January, April, and July months with predicted solar radiation is shown in fig. 7. The actual solar radiation during the selected day of autumn started from 19 w m^{-2} at 7 am then reached 348 w m^{-2} at noon, and declined to 26 w m^{-2} at 5 pm. On the other hand, the predicted solar radiation started from 80 w m^{-2} at 7 am then reached 315 w m^{-2} at noon, and declined to 38 w m^{-2} at 5 pm. The actual solar radiation during the selected day of winter started from 14 w m^{-2} at 8 am then reached 460 w m^{-2} at noon and declined to 43 w m^{-2} at 5 pm. On the other hand, the predicted solar radiation started from 129 w m^{-2} at 8 am then reached 426 w m^{-2} at noon, and declined to 33 w m^{-2} at 5 pm. The actual solar radiation during the selected day of spring started from 41 w m^{-2} at 7 am then reached 792 w m^{-2} at noon, and declined to 51 w m^{-2} at 6 pm. On the other hand, the predicted solar radiation started from 244 w m^{-2} at 7 am then reached 749 w m^{-2} at noon, and declined to 69 w m^{-2} at 5 pm. The actual solar radiation during the selected day of summer started from 10 w m^{-2} at 6 am then reached 683 w m^{-2} at noon, and declined to 12 w m^{-2} at 7 pm. On the other hand, the predicted solar radiation started from 180 w m^{-2} at 6 am then reached 1032 w m^{-2} at noon, and declined to 5 w m^{-2} at 7 pm.

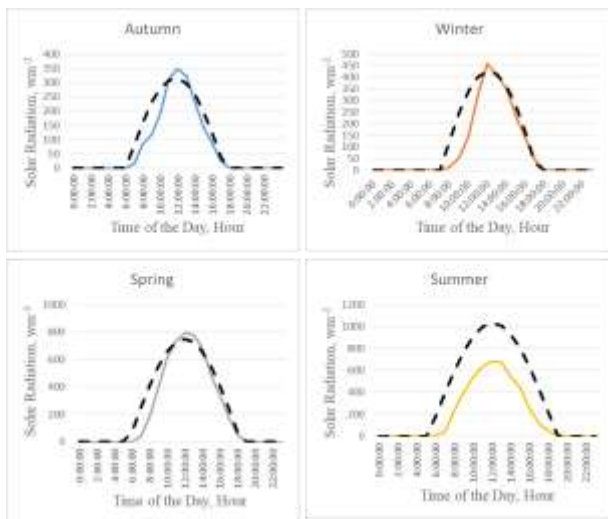


Fig. 7. Hourly actual and predicted solar radiation during autumn, winter, spring, and summer.

The relationships between actual and predicted solar radiation available on the water surface in the outdoor recirculating aquaculture tank for different seasons are shown in fig. 8. It is clear from the equations below (25, 26, 27, and 28) that the maximum coefficient of determination R^2 was in spring (0.9431) then for summer (0.9305) and below them autumn (0.9159) while the lowest was in winter (0.8636).

$$S_P = 1.0053S_A + 16.122 \quad (25)$$

$$S_P = 1.0247S_A + 24.090 \quad (26)$$

$$S_P = 0.9696S_A + 40.149 \quad (27)$$

$$S_P = 1.5498S_A + 73.988 \quad (28)$$

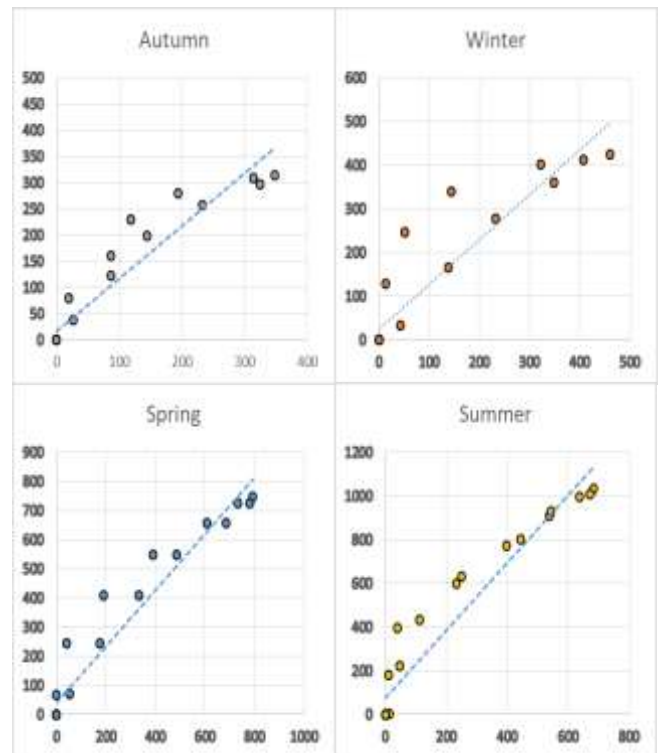


Fig. 8. the relationship between actual and predicted solar radiation available on the water surface in the outdoor recirculating aquaculture tank for different seasons.

3.4.2. Water Temperature

Fig. 9 illustrates the comparison between the predicted and actual water temperature. The predicted temperature of the water in the tank by the model ranged from $21.96 \text{ }^\circ\text{C}$ to $33.26 \text{ }^\circ\text{C}$ with

an average of $27.92 \text{ }^{\circ}\text{C} \pm 1.34 \text{ }^{\circ}\text{C}$. On the other hand, the actual temperature of the water in the tank ranged from 22.20°C to 30.90°C with an average of $28.41 \text{ }^{\circ}\text{C} \pm 1.16 \text{ }^{\circ}\text{C}$.

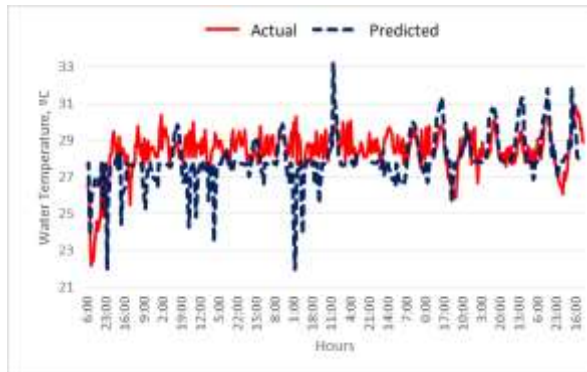


Fig. 9. The predicted and actual water temperature in the tank.

3.4.2. Heat Energy Vectors

Fig. 10 illustrate the relative importance of the most effective energy vectors. The thermal radiation between the water surface and the sky is the most contributor. The solar radiation absorbed by water came as the second contributor. The latent heat loss from the evaporation of the water surface is the lowest contributor. Solar and longwave sky radiation were the two most important influxes of energy for the water tank. The average importance of longwave sky radiation and solar radiation was 27.22% and 20.46%.

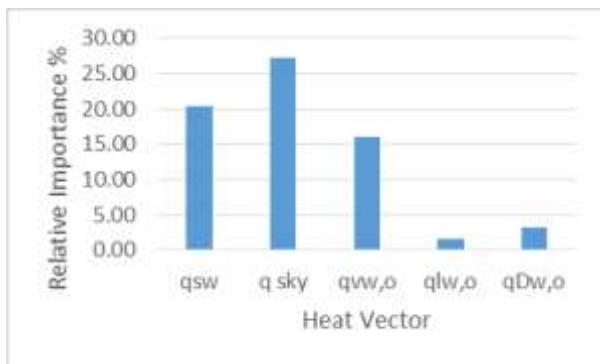


Fig. 10. The relative importance of most effective energy vectors.

DISCUSSION

Solar and longwave sky radiation were the two most important influxes of energy for the water tank. The average importance of longwave sky radiation and solar radiation was 27.22% and 20.46%.

This result agrees with the **Ali (2006)** model result where the average importance of longwave sky radiation and solar radiation were 33% and 21%.

A reasonable difference between the actual and predicted solar radiation especially in winter may be referred to as the cloudiness ratios, which were assumed. The results of the model are similar to the result of the model developed by **Ali (2012)**. The solar radiation on a typical summer day in **Ali's** model was 2402.98 W while it was 2792.62 W in our model. On the other hand, it was 3931.91 W in **Ali's** model while it was 8926.31 W in our model.

The model result is similar to the result obtained by **Khater (2012)**. The model water temperature ranged from $21.96 \text{ }^{\circ}\text{C}$ to $33.26 \text{ }^{\circ}\text{C}$. On the other hand, **Khater's** model temperatures ranged from $24.20 \text{ }^{\circ}\text{C}$ to $29.86 \text{ }^{\circ}\text{C}$ at the same inputs.

The solar radiation absorbed by the water and the thermal radiation between the water surface and the sky is a dominant energy vector such as **Khater (2012)**.

The model of **Li et al. (2009)** concluded that solar radiation is a dominant energy vector while thermal radiation is not the same as us because of the greenhouse cover application in the model.

The difference between the averages of the actual and predicted water temperature is $0.48 \text{ }^{\circ}\text{C}$. While the difference between maximums of the actual and predicted water temperature is $2.36 \text{ }^{\circ}\text{C}$. the difference between minimums of the actual and predicted water temperature is $0.24 \text{ }^{\circ}\text{C}$. The reported best scenario by **Davison and Piedrahita (2015)** resulted in a temperature increase of approximately $3 \text{ }^{\circ}\text{C}$.

The results proved that the model is reliable and valid for the prediction of solar radiation, water temperature, and heat energy required to be added or removed from the water tank concerning Nile tilapia raising in RAS. The model needs to be investigated by doing another validation test with other RASs with different operation variables. It is possible to conduct other experiments inside building greenhouses with one and two covers to validate the model by a wide range of RASs.

Conclusion

A mathematical model was conducted to expect the solar radiation, water temperature, and heat energy required to be added or removed from

RAS'S water tank for Nile tilapia raising, given information about the weather and RAS characteristics. The model estimated the positive and negative energy aspects, which needed to be balanced to control the water tank temperature. The model was developed on a python program with some packages. The product of the work is a stand-alone graphical user interface (GUI) and was named as RAS design and operation assistant. The produced GUI will be available online for any farmer, engineer, researcher, and designer for use and development. At different air temperatures, latitude, longitude, and any weather conditions, the model was able to expect solar radiation, water temperature, and heat energy required to be added or removed. The model predictions and the actual values agreed.

ACKNOWLEDGMENT

The authors want to thank Ahmed I. El-Manawy for his effort in programming and coding in the Python program.

REFERENCES

- Ali, S.A. (2006).** Simulation Model for Aquaculture Pond Heat Balance: I model Development. *Misr Journal of Agricultural Engineering*, 23(1):232–258.
- Ali, S.A. (2012).** Modeling of solar radiation available at different orientations of greenhouses. *Misr Journal of Agricultural Engineering*, 29(3):1181–1196.
- ASHRAE (2009).** *Handbook Heating, Ventilating, and Air-Conditioning Application*; ASHRAE (American Society of Heating, Refrigerating and Air-Conditioning Engineers); Atlanta, GA, USA.
- Davison, A.V. and Piedrahita, R.H. (2015).** Temperature modeling of a land-based aquaculture system for the production of *Gracilar Pacifica*: Possible system modifications to conserve heat and extend the growing season. *Aquac. Eng.* 66:1–10.
- Duffie, J.A.; Beckman, W.A. and Blair, N. (2020).** Solar engineering of thermal processes, photovoltaics and wind. John Wiley & Sons.
- Jain, D. (2007).** Modelling the thermal performance of an aquaculture pond heating with greenhouse. *Build. Environ.*42:557–565.
- Khater, E.G. (2012).** Simulation model for design and management of water recirculating systems in aquaculture (PH.D. thesis). Agricultural Engineering Department, Faculty of Agriculture, Moshtohor, Benha University: Moshtohor, Egypt.
- Li, S.; Willits, D.H.; Browdy, C.L.; Timmons, M.B. and Losordo, T.M. (2009).** Thermal modeling of greenhouse aquaculture raceway systems. *Aquac. Eng.* 42:1–13.
- Lienhard IV, J.H. and Lienhard, J.H.V. (2003).** A Heat Transfer Textbook. Phlogiston Press, Cambridge, MA.
- Makinia, J.; Wells, S.A. and Zima, P. (2005).** Temperature modeling in activated sludge systems: a case study. *Water Environment Research* 77:525–532.
- Papadakis, G.; Frangoudakis, A. and Kyritsis, S. (1992).** Mixed, forced and free-convection heat-transfer at the greenhouse cover. *Journal of Agricultural Engineering Research* 51(3):191–205.
- Ragab, A.M.; El-Gindy, A.M.; Kaddour, O. and Ali, S.A. (2022).** Dissolved Oxygen and Ammonia Mass Balance in a Recirculating Aquaculture System for Raising the Nile Tilapia. *Egyptian Journal of Aquatic Biology and Fisheries*, 26(2):217-237.
- Sarkar, B. and Tiwari, G.N. (2006).** Thermal modeling and parametric studies of a greenhouse fish pond in the Central Himalayan Region. *Energy Conversion and Management* 47:3174–3184.
- Sedory, P.E. (1992).** A dynamic model for the prediction of waste water aeration basin temperature. (MS thesis). UCLA.
- Singh, S. and Marsh, L.S. (1996).** Modeling thermal environment of a recirculating aquaculture facility. *Aquaculture* 139:11–18.
- Swinbank, W.C. (1963).** Long-wave radiation from clear skies. *Quarterly Journal of the Royal Meteorological Society* 89(381):339–348.
- Talati, S.N. and Stenstrom, M.K. (1990).** Aeration-basin heat loss. *J. Environ. Eng.* 116:70–86.
- Zhu, S.; Deltour, J. and Wang, S. (1998).** Modeling the thermal characteristics of greenhouse pond systems. *Aquacultural Engineering* 18:201–217.